

Sub-picosecond ultra-low frequency passively mode-locked fiber laser

Christian Cuadrado-Laborde^{1,2,3} · José L. Cruz¹ · Antonio Díez¹ · Miguel V. Andrés¹

Received: 18 August 2016 / Accepted: 12 October 2016
© Springer-Verlag Berlin Heidelberg 2016

Abstract We developed a nonlinear polarization rotation all-fiber mode-locked erbium-doped fiber laser, with the purpose to reach a sub-picosecond and sub-megahertz light pulse emission. In the process, we observed three different emission regimes as the net birefringence is changed, namely high-power dissipative soliton resonance, low-power soliton regime, and a mixed combination of both. In the pure solitonic regime, a 0.961 MHz train of chirp-free Gaussian pulses was obtained, with a time width of 0.919 ps at 1564.3 nm.

1 Introduction

Ultra-low frequency train of ultrashort light pulses—typically <1 MHz and <1 ps, respectively—is demanded for many applications such as micromachining, biomedicine, and lidar systems. As an example, in ophthalmic surgery, the repetition rate of light pulses is constrained to the multi-kHz region in order to avoid detrimental secondary effects

or to take advantage of high gain regenerative amplifiers [1]. Further, for applications involving materials or tissue removal, laser-induced damage studies show that the damage threshold fluence has a material-dependent optimum in the range 0.1–10 ps [2]. Indeed, conventional mode-locked fiber lasers can provide ultrashort light pulses, but with frequencies well in the ten of MHz and beyond. Solutions encompassing acousto-optic modulators or pocket cells used as pulse pickers to reduce the repetition rate are energetically inefficient. Not to mention that they increase the energy losses impairing the signal-to-noise ratio while simultaneously increasing system's complexity. On the other hand, *Q*-switched lasers fulfill the ultralow frequency requirement, but their pulses widths are well in the nanosecond regime and beyond. Thus, the study of ultrashort and ultralow frequency light pulses is a highly demanded challenging topic.

In fiber lasers, the repetition rate can be easily reduced just by lengthening the cavity, since both are inversely related. In this regard, the advantages of an optical fiber cavity are self-evident, because in solid-state lasers it would be necessary a critical alignment, which can be very cumbersome and time-consuming for long propagation distances. Different results on passively mode-locked fiber lasers with long and ultra-long cavities have been reported. However, lengthening of the fiber cavity increases dispersion; therefore, the temporal width of light pulses obtained is well in the nanosecond regime [3–5]. The waveforms obtained from these lasers are typically Gaussian or hyperbolic secant. In all- and net-normal long dispersion cavities, noise-like or double (temporal)-scale pulses have been also reported [6–8]. Recently, square-shaped pulses were also reported in long-cavity fiber lasers. This phenomenon, known as dissipative soliton resonance (DSR), is governed by the cubic–quintic Ginzburg–Landau equation [9]. By

Electronic supplementary material The online version of this article (doi:10.1007/s00340-016-6548-z) contains supplementary material, which is available to authorized users.

✉ Christian Cuadrado-Laborde
christian.cuadrado@uv.es

¹ Departamento de Física Aplicada y Electromagnetismo, ICMUV, Universidad de Valencia, C/Dr. Moliner, 50, 46100 Burjassot, Spain

² Instituto de Física Rosario (CONICET-UNR), Blvr. 27 de Febrero 210bis, S2000EZP Rosario, Santa Fe, Argentina

³ Facultad de Química e Ingeniería, Pontificia Universidad Católica Argentina, Av. Pellegrini 3314, 2000 Rosario, Argentina

using the nonlinear polarization rotation (NPR) mode-locked technique, square-shaped pulses operating in the DSR regime have been experimentally investigated in fiber ring lasers with normal and anomalous dispersion [10–14]. The generation of rectangular pulses was demonstrated also at net-anomalous dispersion in ring-cavity fiber lasers [12–14]. The dynamics of laser generation have resulted richer at all- and net-anomalous dispersions than at all- and net-normal dispersions. In Ref. [12], a fiber laser was studied, with a ring cavity with total length of 720 m. This laser exhibits a pump power-dependent bi-stable dynamics, from pure soliton-like to mixed DSR soliton-like, as the pump power increases. Unfortunately, the dispersion characteristics were not fully specified, but the dispersion parameter $D \sim 16$ ps/nm km, and the total group velocity dispersion $GVD_T \sim -14.7$ ps², i.e., largely anomalous. In an attempt to reduce the cavity dispersion, a highly nonlinear fiber (HNF) was incorporated in Refs. [13, 14]. Thus, in Ref. [13] a mode-locked NPR fiber laser was presented whose cavity included a 420-m-long HNF (total cavity length 460 m); here, $D = 2.7$ ps/nm km and $GVD_T = -1.582$ ps². A pure soliton-like behavior was reported, with output light pulses in the sub-picosecond regime [13]. A similar approach was followed in Ref. [14], except for the cavity length which was increased up to 1180 m; the average cavity dispersion remained practically invariant as compared with Ref. [13] ($D = 2.54$ ps/nm km), whereas $GVD_T = -3.823$ ps². In this case, the reported dynamics was radically different: typically DSR, with square-shaped light pulses whose minimum time width was 10 ns.

In this work, we experimentally study an ultra-low frequency NPR mode-locked fiber laser. We found essential to use a large effective area fiber (LEAF) in our cavity, which kept both the dispersion and nonlinear effects simultaneously low. We experimentally observe three different regimes, namely pure strong DSR emission, pure weakly soliton-like emission, and a mixed combination of both, as the polarization controller is changed. In the pure solitonic regime, a 961 kHz train of chirp-free Gaussian pulses was obtained, with a time width of 919 fs at 1564.3 nm.

2 Experimental setup

The setup of the passively mode-locked fiber ring laser is schematically illustrated in Fig. 1. The gain was provided by 2.5 m of an erbium-doped, single-clad, optical fiber (EDF) [I-25 by Fibercore®, peak absorption 36.53 dB/m at 1530 nm, cutoff wavelength of 910 nm, and numerical aperture of 0.23]. The EDF was pumped through a 980/1550-nm wavelength division multiplexer (WDM) by a 978-nm pigtailed laser diode, providing a maximum pump power of 600 mW. Next, and following an anticlockwise direction,

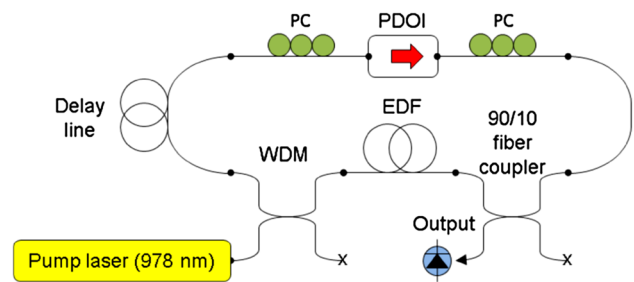


Fig. 1 Setup of the NPR mode-locked fiber laser

the EDF was spliced to the 90 % port of a 90/10 fiber coupler. The input port of the fiber coupler was in turn spliced to the output port of a polarization-dependent optical isolator (PDOI) [dual stage, center wavelength 1550 nm, extinction ratio ≥ 28 dB]. Next, an optical fiber delay line was spliced to the input port of the PDOI. The inclusion of the optical fiber delay line within the cavity has the purpose to increase the total cavity length and consequently allowing the emission of pulses at sub-megahertz repetition rate. Finally, the cavity was closed by connecting the remaining port of the optical fiber delay line to the 1550-nm port of the WDM. Additionally, two manual fiber polarization controllers (PC) were also included, before and after the PDOI. It is worth remarking that the full cavity was constructed with standard commercially available nonpolarization-maintaining fiber components, except of course for the PDOI itself. The output of this laser is obtained from the 10 % port of the optical coupler. The output light pulses were monitored by using a >63-GHz sampling oscilloscope provided with a fast built-in photodetector (53 GHz), real-time oscilloscope (2.5 GHz bandwidth), autocorrelator (scanning range >175 ps, resolution <5 fs, sensitivity 1×10^7 W²), and optical spectrum analyzer (wavelength resolution ± 20 pm).

Since our purpose was the emission at sub-megahertz repetition rate, we incorporate a 204-m-long Corning® LEAF® optical fiber as delay line (numerical aperture 0.14, dispersion parameter 6 ps/nm km). The optical fiber used in the PCs is also Corning LEAF, and its length is included above. The dispersion parameters of the remaining fibers within the cavity include: -22 ps/nm km (EDF), -20 ps/nm km (fiber pigtailed of the WDM, HI1060 Flex fiber, 2 m long), 18 ps/nm km (fiber pigtailed of the fiber coupler, SMF-28e, 2 m long), and 3 ps/nm km (fiber pigtailed of the PDOI, PM 1550 panda fiber, 2 m long). Therefore, the resultant cavity length is 213 m, with average anomalous dispersion $D = 5.5$ ps/nm km, and $GVD_T = -1.513$ ps². Each PC consists of three fiber coils, each held by a plate, which can be rotated around the input fiber's axis. By adjusting its relative orientation, a given input polarization state can be transformed into any output polarization state.

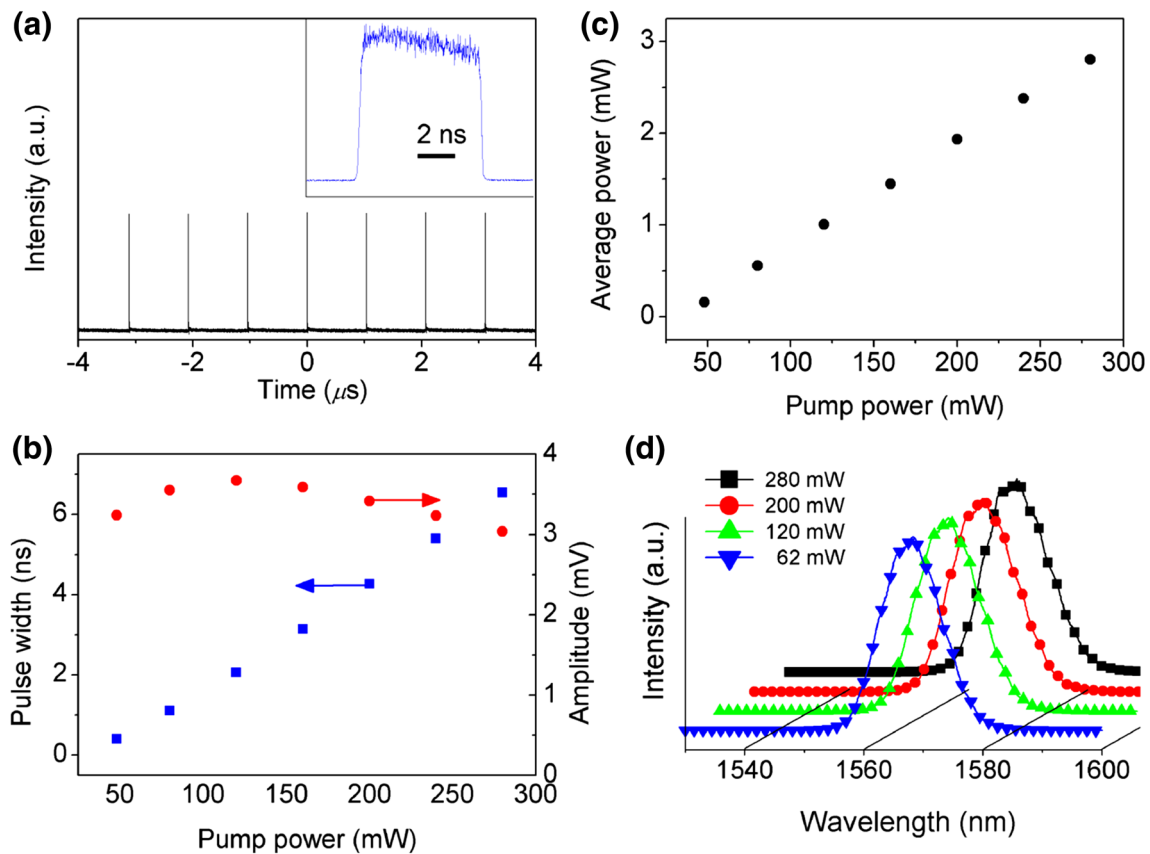


Fig. 2 **a** Train of light pulses at the output of the mode-locked laser with a fundamental frequency of 961 kHz; the inset shows a detail of one of these DSR light pulses for a pump power of 280 mW. **b** Evolution of the pulse width and height as a function of the pump power. **c**

Measured average power as a function of the pump power. **d** Optical spectra for different pump powers (in linear scale and normalized to unity)

In this laser, mode locking is achieved by employing the NPR technique. The PDOI and the PC's drive the unidirectional operation of the laser and concurrently act as the polarization selector in the NPR technique.

3 Results and discussion

Since the proposed laser system has a net-anomalous dispersion, two soliton-shaping mechanisms may eventually be exploited. One is the balance between the anomalous dispersion and the nonlinear Kerr effect and hence the conventional soliton-like pulses generation. The second originates from the balance between gain and loss, resulting in the DSR light pulses generation. In the following, we describe the laser operation.

First, the pump power was raised to 300 mW, which corresponds to the maximum transmittable CW power of the PDOI. Then, a trace is searched in the oscilloscope display by rotating the relative positions of both PC paddles. Usually, a pulsed emission is rapidly found after a

few adjustments. In this situation, the laser typically emits in the DSR regime. Figure 2a shows a typical DSR train; the measured repetition rate was of 961 kHz, which corresponds to the fundamental harmonic mode for a cavity length of 213 m. In Fig. 2a, it is also shown an inset with a detail of one pulse from the train, with the characteristic square-shaped waveform of DSR. The evolution of the pulse width and height as a function of the pump power is shown in Fig. 2b. This behavior of pulse duration increment, and practically invariant pulse height, as the pump power increases, is typical of DSR emission. The minimum pulse width found in this regime was of 370 ps, for a pump power of 44 mW; further pump power reduction induces pulse breakup. Figure 2c shows the measured average power as a function of the pump power, the maximum peak power resulted in 440 mW, for a pump power of 280 mW. Finally, Fig. 2d shows several spectra for different pump powers. It can be observed that the spectral emission did not show an appreciable change as the pump power varies, which is also a distinctive feature of DSR emission [10]. The measured spectral FWHM was of 12.2 nm, with a

maximum variation of 3 % as the pump power changes in the specified range. Usually, NPR mode-locked fiber lasers with medium cavity lengths, i.e., between 100 m and 1 km, are not very reliable to provide stable single-pulse lasing [15]. However, we should stress that once the condition for DSR emission is achieved, this laser system is stable on a laboratory time scale, and any variation of pump power within the range 40–280 mW did not require any readjustment of the PCs.

When the PC paddles were slightly adjusted from the preceding position, the DSR pulses were preserved, but with the irruption of a second signal of considerably lower intensity at an undefined frequency, which can be described as a train of pulses with constant pulse peak power, but not defined repetition rate. Figure 3a shows the typical trace of this regime in a real-time oscilloscope. The first thing that caught the attention, being determinant to identify this special regime through the oscilloscope trace, is the constant pulses' intensity of this second signal, which is one order of magnitude smaller than the train of high-peak-power pulses. The high intensity peaks at 961 kHz are the DSR pulses, with similar characteristics as explained above, whereas the lower intensity peaks could not be adequately

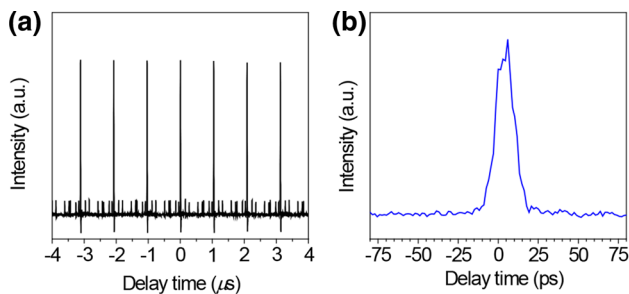
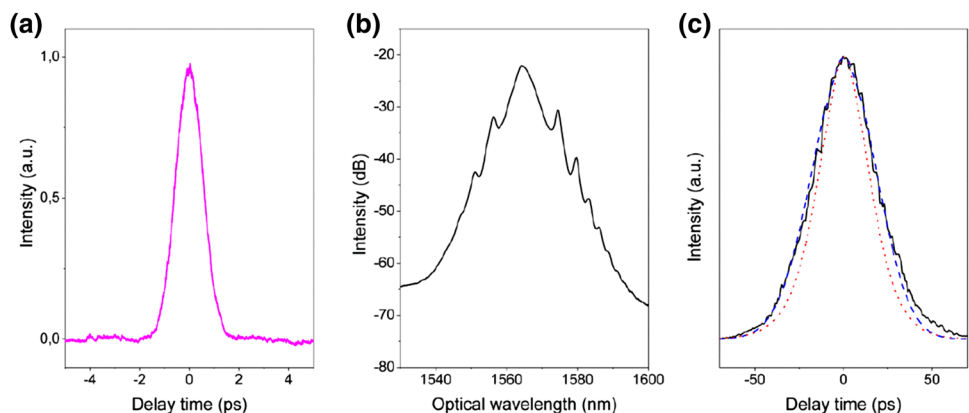


Fig. 3 **a** Real-time oscilloscope trace showing the coexistence of DSR light pulses together with soliton-like pulses, for a pump power of 120 mW. **b** Detail of one of the short soliton-like pulses between the high intensity DSR pulses measured with a 50-GHz sampling oscilloscope

resolved at this stage. Hence, we decided to resolve them with the sampling oscilloscope; the measured signal is shown in Fig. 3b. Since the measured time width of these weaker pulses (12 ps) is below the temporal resolution of our sampling oscilloscope, these pulses would be actually shorter. The behavior of these short pulses was typically solitonic, in the sense that an increment of the pump power does not raise their peak power, but is used to generate a new short pulse, owing to the energy quantization condition. Thus, we identified this particular operation point as a mixed regime, where coexist DSR and multi-soliton-like pulses. On the other hand, a real-time recording (obtained expanding the time window to several round-trip times, while simultaneously preserving the temporal resolution) reveals slow internal motions of soliton-like pulses inside the condensed phase, which have been compared to a liquid state [16]. Therefore, one strong DSR light pulse coexists with multiple weak soliton-like pulses within the laser cavity at this particular birefringence state. The coexistence of strong and weak pulses in this kind of fiber lasers was also reported in Ref. [12], as the pump power increases above a given threshold. However, in this case the coexistence can be obtained in a one order of magnitude lower net-anomalous dispersion and as a function of the polarization adjustment.

Further change of the polarization controllers through another slight adjustment of the paddles gives origin to the third regime. In this regime, the soliton-like train is preserved, whereas, simultaneously, the DSR train is completely annihilated. According to the experimental observations, there is one single soliton-like pulse per round-trip time, when the pump power is restricted to a narrow band around 41 mW. Figure 4a shows the trace of the measured intensity autocorrelation, with a measured FWHM of 1.30 ps. If we assume a hyperbolic secant waveform for the emitted light pulse, this translates in a pulse width of 842 fs (decorrelation factor: 0.648). However, since the laser cavity is not fully anomalous, but mixed, it would be more accurate to refer to these short pulses as dispersion-managed solitons, whose pulse shape is closer to

Fig. 4 Intensity autocorrelation and optical spectrum, **(a)** and **(b)**, respectively, when the laser emits in the pure soliton-like regime. **c** Measured pulse after propagation by a dispersive line (*solid black curve*), together with the simulated responses: Gaussian (*dashed blue curve*) and hyperbolic secant (*dotted red curve*)



being Gaussian rather than hyperbolic secant [17]. Therefore, by assuming a Gaussian profile for the emitted light pulses, this translates in a pulse width of 919 fs (decorrelation factor: 0.707). The measured average power was of 0.13 mW, whereas the peak power was of 147 W. This represents around 130 pJ of pulse energy, which is usual for standard fibers [10, 12]. On the other hand, the measured spectrum is typically soliton-like, i.e., with spectral sidebands corresponding to the dispersive waves, see Fig. 4b [17]. The measured -3 -dB bandwidth was 4.66 nm (central wavelength 1564.3 nm), which corresponds to 0.55 THz at the central frequency of 191.64 THz. Therefore, these soliton-like pulses have a time bandwidth product $TBP = 0.55 \text{ THz} \times 842 \text{ fs} = 0.46$, or $TBP = 0.55 \text{ THz} \times 919 \text{ fs} = 0.5$, when either a hyperbolic secant or Gaussian shapes are assumed, respectively. In this sense, the output light pulses would be closer to be Gaussian (whose theoretical $TBP = 0.44$) than to be hyperbolic secant (theoretical $TBP = 0.315$). We intended to confirm this assumption, by propagation of the emitted soliton-like pulses through a dispersive line, with the purpose to measure its true temporal profile with our sampling oscilloscope. In Fig. 4c is shown the measured temporal waveform, together with the simulated propagations of a hyperbolic secant and Gaussian pulses by the dispersive line (SMF-28 fiber, 656 m long). In the simulations, the field amplitude of the light pulse at the input of the dispersive line was approximated by the following expressions: $\text{sech}(t/T_0)$ and $\exp(-t^2/2T_0^2)$, where T_0 is the temporal half-width at $1/e$ intensity point (related with the FWHM through $T_{\text{FWHM}} \cong 1.763T_0$ and $T_{\text{FWHM}} \cong 1.665T_0$, for the hyperbolic secant and Gaussian shapes, respectively). Therefore, by using the intensity autocorrelation measurement, in the hyperbolic secant case $T_{\text{FWHM}} = 842 \text{ fs}$, then $T_0 = 477 \text{ fs}$, whereas for the Gaussian case $T_{\text{FWHM}} = 919 \text{ fs}$, then $T_0 = 552 \text{ fs}$. Further, since the spectral bandwidth of the light pulses under study is nonnegligible, the variation of the first order dispersion D as a function of the optical wavelength was taken into account, which can be approximated by $D(\lambda) = S_{\text{ZD}}(\lambda - \lambda_{\text{ZD}}^4/\lambda^3)/4$ where $\lambda_{\text{ZD}} = 1313 \text{ nm}$ is the zero-dispersion wavelength and $S_{\text{ZD}} = 0.086 \text{ ps/nm}^2 \text{ km}$ is the zero-dispersion slope. The inclusion of a third order dispersion term might not be necessary, since the central wavelength of the pulse under analysis is not close to λ_{ZD} . It can be observed from Fig. 4c that the Gaussian pulse better matches the experimental measurement than the hyperbolic secant pulse, confirming our assumption. Further, since this matching was reached without including any additional phase term in the simulated input pulse, we conclude that our soliton-like pulses are chirp-free. It is worth saying also that this soliton-like emission was found only at a very specific orientation of the PC plates, which is in accordance with previous theoretical work [12], and simultaneously could explain its elusive nature. Once the angles of input and output polarization controllers are found, the laser emits with a reasonable stability, for an

ordinary laboratory environment. In this regime, the soliton-like number in the cavity increases with the increase in pump power, whereas the peak and duration of each soliton-like do not appreciable changes. Coupling of two, three, or more solitons was observed. Here, the solitonic emission could be obtained at different dispersion regimes when the LEAF fiber was shortened; e.g., at 1.8 MHz fundamental cavity frequency; as opposed to results reported in Ref. [12], where the achievement of the hyperbolic secant solitons implied cumbersome adjustments between the EDF and SMF lengths. We should point out also that in our laser the soliton pulses are more than three times shorter than in Ref. [12] and have three times more energy per pulse, so the peak power of the pulses is about 10 times higher. Finally, in the supplementary material (Video 1), we provide an enlighten short laboratory film showing the whole evolution from pure soliton-like to DSR, through the mixed soliton-like DSR regime, just by carefully adjusting the PCs for a fixed pump power of 160 mW.

4 Summary

Thus, using standard telecommunication fibers and commercially available fiber-optic components, we developed a simple all-fiber mode-locked erbium-doped fiber laser. We observed three different emission regimes as the polarization controller is changed, namely pure strong DSR emission, pure weakly soliton-like emission, and a mixed combination of both. In the pure solitonic regime, a 961 kHz train of chirp-free Gaussian pulses was obtained, with a time width of 919 fs at 1564.3 nm. Such ultra-low repetition rate as well as short pulse width makes this mode-locked all-fiber laser a suitable oscillator to directly seed a fiber amplifier, which can be used as compact sources for high-power applications.

Funding The authors acknowledge financial support from the *Ministerio de Economía y Competitividad* of Spain and the *Fondo Europeo de Desarrollo Regional* (FEDER)—Project TEC2013-46643-C2-1-R—and the *Generalitat Valenciana*—Project PROMETEOII/2014/072. The work of C. Cuadrado-Laborde has been partially supported by CONICET and ANPCyT (Projects PIP112-2015-0100607-CO and PICT-2015-2818, respectively), Argentina.

References

1. T. Juhasz, F.H. Loesel, R.M. Kurtz, C. Horvath, J.F. Bille, G. Mourou, Corneal refractive surgery with femtosecond lasers. *IEEE J. Sel. Top. Quant.* **5**(4), 902–910 (1999)
2. A. Tien, S. Backus, H. Kapteyn, M. Murnane, G. Mourou, Short-pulse laser damage in transparent materials as a function of pulse duration. *Phys. Rev. Lett.* **82**(19), 3883–3886 (1999)
3. S. Kobtsev, S. Kukarin, Y. Fedotov, Ultra-low repetition rate mode-locked fiber laser with high-energy pulses. *Opt. Expr.* **16**(26), 21936–21941 (2008)

4. A. Ivanenko, S. Kobtsev, S. Smirnov, A. Kemmer, Mode-locked long fibre master oscillator with intra-cavity power management and pulse energy $>12 \mu\text{J}$. *Opt. Expr.* **24**(6), 6650–6655 (2016)
5. B. Nyushkov, V. Denisov, S. Kobtsev, V. Pivtsov, N. Kolyada, A. Ivanenko, S. Turitsyn, Generation of 1.7- μJ pulses at 1.55 μm by a self-mode locked all-fiber laser with a kilometers-long linear-ring cavity. *Laser Phys. Lett.* **7**(9), 661–665 (2010)
6. S. Smirnov, S. Kobtsev, S. Kukarin, A. Ivanenko, Three key regimes of single pulse generation per round trip of all-normal-dispersion fiber lasers mode-locked with nonlinear polarization rotation. *Opt. Expr.* **20**(24), 27447–27453 (2012)
7. S. Kobtsev, S. Smirnov, S. Kukarin, S. Turitsyn, Mode-locked fiber lasers with significant variability of generation regimes. *Opt. Fiber Technol.* **20**(6), 615–620 (2014)
8. D. Churkin, S. Sugavanam, N. Tarasov, S. Khorev, S. Smirnov, S. Kobtsev, S. Turitsyn, Stochasticity, periodicity and localized light structures in partially mode-locked fibre lasers. *Nature Commun.* **6**, 7004 (2015)
9. N. Akhmediev, J.M. Soto-Crespo, P. Grelu, Roadmap to ultra-short record high-energy pulses out of laser oscillators. *Phys. Lett. A* **372**, 3124–3128 (2008)
10. X. Liu, Pulse evolution without wave breaking in a strongly dissipative-dispersive laser system. *Phys. Rev. A* **81**(5), 053819 (2010)
11. X. Wu, D.Y. Tang, H. Zhang, L.M. Zhao, Dissipative soliton resonance in an all-normal dispersion erbium-doped fiber laser. *Opt. Expr.* **17**(7), 5580–5584 (2009)
12. X. Liu, Coexistence of strong and weak pulses in a fiber laser with largely anomalous dispersion. *Opt. Expr.* **19**(7), 5874–5887 (2011)
13. C. Jiong, J. Dong-Fang, W. Yong-Chao, W. Chang-Le, W. Zhao-Ying, Y. Tian-Xin, Passively mode-locked fiber laser with a sub-megahertz repetition rate. *Chin. Phys. Lett.* **28**(11), 114203 (2011)
14. X. Zhang, C. Gu, G. Chen, B. Sun, L. Xu, A. Wang, H. Ming, Square-wave pulse with ultra-wide tuning range in a passively mode-locked fiber laser. *Opt. Lett.* **37**(8), 1334–1336 (2012)
15. S. Kobtsev, S. Smirnov, Fiber lasers mode-locked due to nonlinear polarization evolution: golden mean of cavity length. *Laser Phys.* **21**(2), 272–276 (2011)
16. F. Amrani, M. Salhi, P. Grelu, H. Leblond, F. Sanchez, Universal soliton pattern formations in passively mode-locked fiber lasers. *Opt. Lett.* **36**(9), 1545–1547 (2011)
17. G.P. Agrawal, *Nonlinear fiber optics*, 3rd edn. (Academic Press, San Diego, 2001)